

# Kinematics and Dynamics Modelling of a Mecanum Wheeled Mobile Platform

Nkgatho Tlale

Council for Scientific and Industrial Research  
Pretoria, RSA  
Email: ntiale@csir.co.za

Mark de Villiers

Council for Scientific and Industrial Research  
Pretoria, RSA  
Email: mfdevilliers@csir.co.za

**Abstract**—Omni-directional mobile platforms have the ability to move instantaneously in any direction from any configuration. As such, it is important to have a mathematical model of the platform, especially if the platform is to be used as an autonomous vehicle. Autonomous behaviour requires that the mobile robot choose the optimum vehicle motion in different situations for object/collision avoidance and task achievement. This paper develops and verifies a mathematical model of a mobile robot platform that implements mecanum wheels to achieve omni-directionality. The mathematical model will be used to achieve optimum autonomous control of the developed mobile robot as an office service robot. Omni-directional mobile platforms have improved performance in congested environments and narrow aisles, such as those found in factory workshops, offices, warehouses, hospitals, etc.

**Index Terms**—Automated guided vehicle; mecanum wheels; omni-directionality; kinematics modelling; dynamics modelling

## I. INTRODUCTION

Automated guided vehicles (AGVs)/ mobile platforms are used extensively in reconfigurable manufacturing systems (RMS) for materials handling [1]. Omni-directionality is the ability of a mobile platform to move instantaneously in any direction from any configuration. The mobile platform used in this project implements mecanum wheels, which are special wheel designs that are based on a concept that achieves traction in one direction and allows passive motion in another. This allows greater flexibility in congested environments [2]. For certain motions of the mobile platform, mecanum wheels allow the mobile platform to change its direction of motion without changing its orientation. Design of the mecanum wheel can be found in Dickerson and Lapin [3]. The centralized controller design of a mecanum wheel AGV was addressed by [3], while Tlale [4] addressed its distributed controller design. The overall motion of the mecanum wheel can be thought of as the resultant motion of the screw when turned, with the threads being rollers and only one or two threads making contact with ground at only one point along the length of the thread.

Mecanum wheels consist of a number of rollers (eight rollers in our case) around the circumference of the wheel hub. The rollers are orientated at some angle,  $\alpha$ , from the axis of rotation of the wheel. In our case  $\alpha = 45^\circ$ . Rollers, in turn, can rotate about their own axis. When the mecanum wheel is rotating, at most two rollers and least one roller are/is

in contact with the ground. Only a small surface of the roller makes contact with the ground [5]. The area making contact with the ground transverses from one side of the roller to the other side, depending on the direction of the rotation of the mecanum wheel. Traction is obtained along the direction of  $\alpha$  depending on the rotational direction of the mecanum wheel, which influences the movement of the direction of the area making contact with the ground (refer Fig. 4). From this description, the effective rotational velocity of the mecanum wheel is determined as:

$$\dot{\theta} = n\dot{\theta}_m \sin \alpha \quad (1)$$

where  $\dot{\theta}_m$  is the rotational velocity of the DC motor that is driving the mecanum wheel and  $n$  is the gear ratio of the DC motor driving the mecanum wheel.

The rotational velocity of each wheel can be found from encoder pulses of each wheel as follows:

$$\dot{\theta} = C \frac{\Delta m}{\Delta T} \quad (2)$$

where  $\dot{\theta}$  is the rotational velocity of the mecanum wheel,  $C$  is a constant that is dependant on the number of pulses per encoder revolution, the radius of the mecanum wheels and the gear ratio of the DC motors used,  $\Delta m$  is the change in the number of encoder pulses for wheel and  $\Delta T$  is the time interval of sampling encoder pulses.

The effectiveness of the motor,  $e$ , in converting the driving motor's rotational velocity into useful velocity, using the mecanum wheel, can be defined as:

$$e = \frac{\dot{\theta}}{n\dot{\theta}_m} = \sin \alpha \quad (3)$$

This indicates that when rollers are mounted parallel to the axis of rotation of the mecanum wheel, negligible motion will be achieved as the rollers will be producing only wheel slip. When the rollers are mounted perpendicular to the axis of rotation of the mecanum wheel, maximum motion will be produced. Whenever the relationship in (1) does not hold, slip is being experienced. Slip is mainly caused by rollers rotation around their shafts while the wheel is rotating. Slip is defined by the following relationship:

$$s = \frac{d_r}{d} = \frac{d_r}{rn\dot{\theta}\Delta T \sin \alpha} \quad (4)$$

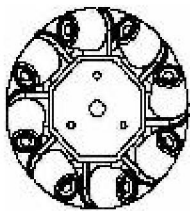


Fig. 1. Mecanum wheel design with centrally mounted rollers which can rotate about their own axis to reduce friction [5]

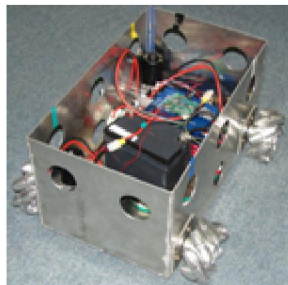


Fig. 2. Mobile test platform

where  $d_r$  is the real displacement of the mobile platform in a measured time interval  $\Delta T$ ,  $r$  is the mean outer radius of the mecanum wheel, and  $d$  is the displacement, in the measured time interval, of the mecanum wheel as measured by the inertial sensors of mobile platform measurement system.

In this project, the improved mecanum wheel design, that used rollers which were held in the middle, was implemented. The advantage of this design is that the wheels produced less friction while driving on general surfaces. With free rotating rollers any combinations of forward, sideways and reverse movement are possible with less friction [9]. The developed mobile platform was developed for indoor applications, especially for office automation e.g. mobile platform for delivery of coffee, mail, etc. in an office environment. Fig. 1, 2 and 3 show the mecanum wheel design and the developed mobile robot.

## II. EXPERIMENTAL PLATFORM

Four mecanum wheels were used for the mobile platform in this project. The direction and magnitude of the rotational speed of each wheel was independently controlled. By using the same magnitude of rotational speeds of wheels at the

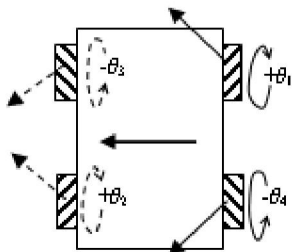


Fig. 3. Typical force motion analysis for mecanum wheeled mobile platform

same time during the operation of the mobile platform, a maximum of eighty-one combinations of wheels (four wheels: 1,2, 3 and 4) and directions of rotational velocity of wheels (three directions of rotation: stationary (0), clockwise ( $+\theta$ ) and counter-clockwise ( $-\theta$ ). Using different rotational directions of the wheels introduced moments on the mobile platform, which tended to make the mobile platform rotate controllably/uncontrollably. This paper models the motion of a mecanum wheel mobile platform with the aim of implementing an autonomous omni-directional mobile platform in an office environment.

To control the resultant direction of the motion of the mobile platform, different relative rotational speeds of different mecanum wheels were used. For example, to move the robot to the left, the right wheels were rotated against each other outwardly; while the left wheels were rotated against each other inwardly (refer Fig. 3). Any desired orientation of the mobile robot could be achieved using the same technique.

When the mobile platform is moving on surfaces having very low friction, such as surfaces covered with oil, low friction plastics, etc, a lot of slip is encountered and the mobile platform cannot be controlled effectively. It sometimes becomes dangerous for the mobile platform to operate in such conditions. It is necessary to detect slip that occurs during such conditions. Moreover, surfaces such as concrete, which have a high coefficient of friction induce high wear on the wheels. So these surfaces are not conducive for operation of the mobile platform.

The developed mobile platform uses a sensor measurement system which is used to verify the mathematical model. The sensor measurement system consists of the following sensors:

- each wheel is fitted with wheel encoder for measuring rotation of the wheel, velocity and acceleration of each wheel
- a 3D gyrometer system in order to measure rotational motion in each axis
- a 3D accelerometer system in order to measure the resultant translational motion in each axis.

## III. MATHEMATICAL MODELLING

In the model that is developed below it is assumed that the mobile platform's frame is rigid and that all the points on the vehicle rotate about the instantaneous centre of rotation. Shimada et. al. [6], Tahboub [7] and Viboonchaicheep et. al [8] developed mathematical models for omni-directional mobile platforms for position control. The model developed in this paper is focused on autonomous control of mecanum wheeled mobile platform.

### A. Dynamics Modelling

Fig. 4 shows the forces acting on a single roller instantaneously in contact with the surface under the mobile platform.  $F_{Ti}$  is the force developed on the roller due to the motor torque  $T_i$  at the circumference of the mecanum wheel  $i$ . The

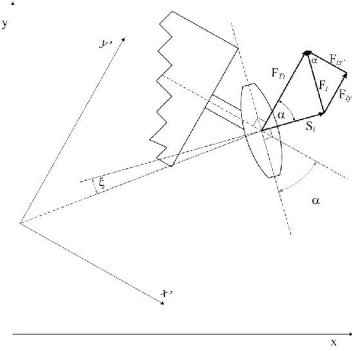


Fig. 4. View of forces acting on the roller in contact with the ground

developed torque can be expressed as:

$$\begin{aligned} T_i &= r\mathbf{F}_{Ti} \\ &= r\mu_d \mathbf{F}_{if} + (I_w + \mu_{dd})\ddot{\theta}_i \end{aligned} \quad (5)$$

where  $\ddot{\theta}_i$  is rotational acceleration of the mecanum wheel  $i$ ,  $\mu_d$  is the coefficient of dynamic friction (between wheel and ground),  $\mu_{dd}$  is the coefficient of viscous friction (between the motor shaft and its bearings),  $\mathbf{F}_{if}$  is the frictional force proportional to the weight of the mobile platform and  $I_w$  is the inertia constant of the wheel about its mass centre.  $\mathbf{F}_{Ti}$  is determined from the DC motor voltage and the current drawn by the motor. The developed force  $\mathbf{F}_{Ti}$  is divided into the roller ineffective slip force,  $\mathbf{S}_i$ , and the effective drive force,  $\mathbf{F}_i$ . The sum of all the effective forces developed at all the wheels creates the motion of the mobile platform. This sum can be shown to be (ignoring frictional forces for now):

$$\sum_{i=1}^4 \mathbf{F}_i = \mathbf{F}_{Ti} \sin \alpha \quad (6)$$

while each slip force developed at each wheel is defined by the following equation:

$$\mathbf{S}_i = \mathbf{F}_{Ti} \cos \alpha \quad (7)$$

Let  $(x, y, z)$  be reference stationary coordinates axis, while  $(x', y', z')$  is body-attached coordinates axis at the geometrical centre of the mobile platform as indicated in Fig. 4 and 5. The components of the effective force,  $\mathbf{F}_i$ , in the body stationary coordinate axis  $(x', y', z')$  are:

$$\mathbf{F}_i = \mathbf{F}_{ix'}\mathbf{i}' + \mathbf{F}_{iy'}\mathbf{j}' \quad (8)$$

where  $\mathbf{i}'$  and  $\mathbf{j}'$  are unit vectors in the directions  $x'$  and  $y'$  respectively. The force  $\mathbf{F}_i$  is co-axial with the roller instantaneously in contact with the surface under the mobile platform. The sum of the components of the forces in the  $x'$ -axis which cause motion of the mobile platform can be shown to be:

$$\begin{aligned} \sum_{i=1}^4 \mathbf{F}_{ix'} &= \sum_{i=1}^4 \mathbf{F}_i \cos \alpha \\ &= \sum_{i=1}^4 (-1)^i (\text{SIG}(\theta_i)) K_i \mathbf{F}_{Ti} \sin \alpha \cos \alpha \end{aligned} \quad (9)$$

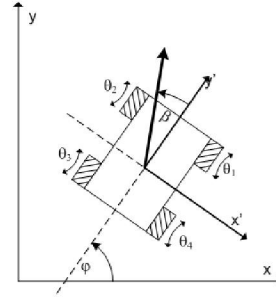


Fig. 5. Mecanum wheeled mobile platform and its coordinates

while the sum of the components in the  $y'$ -axis can be shown to be:

$$\sum_{i=1}^4 \mathbf{F}_{iy'} = \sum_{i=1}^4 \mathbf{F}_i \sin \alpha = \sum_{i=1}^4 (\text{SIG}(\theta_i)) K_i \mathbf{F}_{Ti} i (\sin \alpha)^2 \quad (10)$$

where  $i$  is the wheel number,  $\text{SIG}(\theta_i)$  is the sign representing the rotational direction of wheel  $i$  as determined by the right-hand rule (clockwise = +, and counter-clockwise = -),  $K_i$  is the wheel constant dependant on the number of rollers per wheel and how tight the rollers are on the wheel's hub,  $\theta_i$  is rotational velocity of wheel  $i$ . The direction of the resultant force from all the wheels is the same as the direction of the resultant driving velocity on the mobile platform. Using the stationary reference frame  $(x, y, z)$  and Newton's second law of motion, then the sum of forces causing motion of the mobile platform parallel to the  $x$ -axis is (now adding frictional forces):

$$m\ddot{x} = \sin \varphi \sum_{i=1}^4 \mathbf{F}_{ix'} + \cos \varphi \sum_{i=1}^4 \mathbf{F} - \sum_{i=1}^4 \mathbf{F}_{ifx} \quad (11)$$

which can be expanded to:

$$m\ddot{x} = \sum_{i=1}^4 \left\{ \begin{array}{l} ((-1)^i (\text{SIG}(\theta_i)) K_i \mathbf{F}_{Ti} \sin \alpha \cos \alpha \sin \varphi) \\ + ((\text{SIG}(\theta_i)) K_i \mathbf{F}_{Ti} (\sin \alpha)^2 \cos \varphi) - \mathbf{F}_{ifx} \end{array} \right\} \quad (12)$$

where  $m$  is the total mass of the mobile platform,  $\ddot{x}$  is component of the mobile platform's acceleration in the  $x$ -axis,  $\theta_i$  is the angular rotation made by wheel  $i$ ,  $\mathbf{F}_{ifx}$  is the frictional force developed on wheel  $i$  in the  $x$ -direction and  $\alpha$  is the angle that the rollers make with the shaft of wheel  $i$ . Similarly, the sum of the components of the effective forces that is developed on the mobile platform parallel to the  $y$ -axis is:

$$m\ddot{y} = \sum_{i=1}^4 \left\{ \begin{array}{l} ((-1)^i (\text{SIG}(\theta_i)) K_i \mathbf{F}_{Ti} \sin \alpha \cos \alpha \cos \varphi) \\ + ((\text{SIG}(\theta_i)) K_i \mathbf{F}_{Ti} (\sin \alpha)^2 \sin \varphi) - \mathbf{F}_{ifx} \end{array} \right\} \quad (13)$$

where  $\ddot{y}$  is the component of the vehicle's acceleration in direction of the  $y$ -axis of the stationary reference coordinate system  $(x, y, z)$ .

The frictional forces developed on the mobile platform can be seen as the sum of the frictional forces on each wheel. The frictional forces on each wheel are dependent on the position of the mass centre relative to the geometric centre

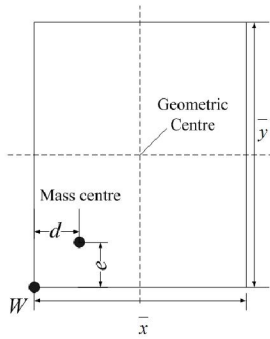


Fig. 6. View of the geometric centre and theoretical position of mass centre

of the mobile platform and the material used on the floor. If the mass centre coincides with the geometric centre, the frictional forces will be equal on each wheel and add up to  $\mathbf{F}_{if}$ . Referring to Fig. 6 the frictional forces developed can be shown to be:

$$\mathbf{F}_{if} = \mu_{ddm} \left( \frac{\bar{y} - e_i}{\bar{y}} \right) \left( \frac{\bar{x} - d_i}{\bar{x}} \right) \quad (14)$$

where  $\bar{y}$  is the distance from the front wheels to the back wheels, or the wheel base, and  $\bar{x}$  is the distance from the left-hand wheels to the right-hand wheels, or the track of the vehicle,  $e_i$  is the offset distance of the mass centre from the centre of wheel  $i$  in the  $y'$  direction and  $d_i$  is the offset distance of the mass centre from the centre of wheel  $i$  in the  $x'$  direction. Both  $e$  and  $d$  always have positive values, otherwise the mass centre falls outside the wheelbase of the vehicle and the vehicle will be unstable. The torque developed on the mobile platform to make its orientation change is:

$$\begin{aligned} \mathbf{T} &= \sum_{i=1}^4 a_i |(\mathbf{F}_i - \mathbf{F}_{if})| \cos \xi_i l_i \\ &= I \ddot{\varphi} \end{aligned} \quad (15)$$

where  $a_i$  is a constant depending on the wheel number and  $a_1 = -1$  for  $i = 1$  and  $4$ , and  $a_2 = a_3 = 1$  for  $i = 2$  and  $3$ ,  $\mathbf{T}$  is the torque developed on the vehicle that changes the posture of the vehicle,  $I$  is the mass inertia of the vehicle in the  $xy$ -plane,  $\ddot{\varphi}$  is the angular acceleration of the vehicle in the  $xy$ -plane which is measured by gyroscope,  $\mathbf{F}_i$  is determined by (8),  $\xi_i$  is the angle that the line from the geometric centre of the vehicle to the centre of wheel  $i$  makes with rollers of that wheel (it is greater than  $90^\circ$  for rectangular wheel set-ups where  $\frac{\bar{y}}{\bar{x}} > 1$ ,  $90^\circ$  for a square setup where  $\frac{\bar{y}}{\bar{x}} = 1$  and less than  $90^\circ$  for rectangular wheel set-ups where  $\frac{\bar{y}}{\bar{x}} < 1$ ),  $l_i$  is the distance from the mass centre to the centre of wheel  $i$  on the  $xy$ -plane which is defined as:

$$l_i = \frac{\sqrt{\bar{x}_i^2 + \bar{y}_i^2}}{2} \quad (16)$$

This equation is only true for rotations about the geometrical mass-centre. For other rotations refer to the next section. Equation (15) does not hold for linear resultant motions where the orientation of the mobile platform does not change.

### B. Kinematics Modelling

The velocity developed at each wheel of the mobile platform, can be defined as follows in the body-attached coordinate axis ( $x'$ ,  $y'$ ,  $z'$ ):

$$\mathbf{v}_i = \text{SIG}(\theta_i) K_i r \dot{\theta}_i \sin \alpha \quad (17)$$

Its direction is in the same direction as the angular orientation of the rollers,  $\alpha$ . The sum of effective velocities in the  $x'$  direction can be shown to be:

$$\begin{aligned} \sum_{i=1}^4 \mathbf{v}_{ix'} &= \sum_{i=1}^4 \mathbf{v}_i \cos \alpha \\ &= \sum_{i=1}^4 (-1)^i \text{SIG}(\theta_i) K_i r \dot{\theta}_i \sin \alpha \cos \alpha \end{aligned} \quad (18)$$

while the sum of the components in the  $y'$  direction can be determined by:

$$\begin{aligned} \sum_{i=1}^4 \mathbf{v}_{iy'} &= \sum_{i=1}^4 \mathbf{v}_i \sin \alpha \\ &= \sum_{i=1}^4 (-1)^i \text{SIG}(\theta_i) K_i r \dot{\theta}_i (\sin \alpha)^2 \end{aligned} \quad (19)$$

The resultant velocity is then defined by:

$$\mathbf{v} = \sum_{i=1}^4 v_{ix'} \mathbf{i}' + \sum_{i=1}^4 v_{iy'} \mathbf{j}' \quad (20)$$

In the global reference coordinates ( $x$ ,  $y$ ,  $z$ ), the velocity of the mobile platform is defined by:

$$\mathbf{v}_x = \sin \varphi \sum_{i=1}^4 \mathbf{v}_{ix'} + \cos \varphi \sum_{i=1}^4 \mathbf{v}_{iy'} \quad (21)$$

and

$$\mathbf{v}_y = \cos \varphi \sum_{i=1}^4 \mathbf{v}_{ix'} + \sin \varphi \sum_{i=1}^4 \mathbf{v}_{iy'} \quad (22)$$

And the direction of the resultant motion,  $\beta$ , in the stationery coordinate axis ( $x$ ,  $y$ ,  $z$ ) is defined by:

$$\beta = \arctan \left( \frac{\mathbf{v}_y}{\mathbf{v}_x} \right) \quad (23)$$

Due to the geometry of the mecanum wheel platform  $\beta$  can be in one of 8 directions, using compass directions for ease of explanation this means that  $\beta$  can be N, NE, E, SE, S, SW, W, NW. The posture of the vehicle is determined by the angle  $\varphi$  which is measured relative to the  $x$ -axis.  $\varphi$  can only be changed with rotational motion, this is handled in the next section.

### IV. TURNING MOTIONS WITH A MECANUM WHEEL PLATFORM

During turning motions, it becomes important to determine the radius of turn of a motion. There are three cases where the vehicle can achieve pure turning motions; where all the four wheels are used, where only three wheels are used, and where only two wheels are used (refer to Fig. 7 to 9, respectively). Theoretically, when only one wheel is used, posture of the vehicle will change. In practice, this is not achieved because of the low driving force developed by one wheel and the relatively large friction produced by the other wheels.

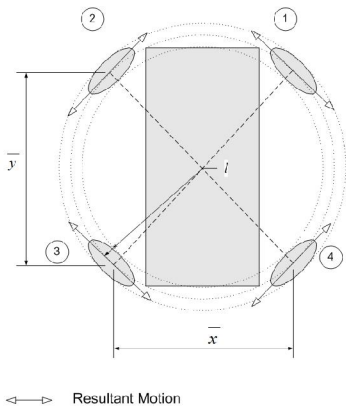


Fig. 7. Rotational motion using all four wheels

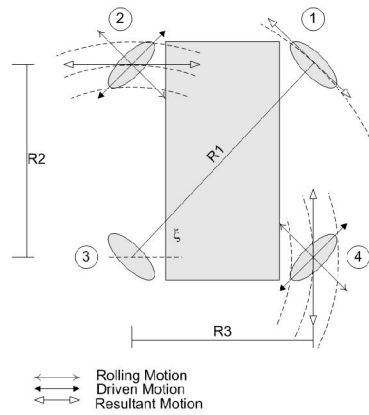


Fig. 8. Rotational motion using driving three wheels

#### A. Four wheel rotation

Rotational motion using all wheels is shown in Fig. 7. When all the wheels have resulting moments that have the same direction about the geometrical centre of the mobile platform; either a clockwise or counter-clockwise motion about the mass centre is achieved. If one wheel produces an opposite moment to the other three, then rotation around a centre outside the vehicle is produced. If two wheels produce opposite moments we return to a linear motion case, except for the two cases where no motion is exhibited. In the pure rotation case around the geometric centre, the rotational velocity  $\dot{\varphi}$  can be shown to be:

$$\dot{\varphi} = \frac{\mathbf{v}_i}{l_i} \quad (24)$$

The rotational velocity of each wheel around the geometric centre is the same, the torque contributions of each wheel are given in (5). For this case there is no motion of the vehicles geometric centre in the global  $xy$ -plane.

#### B. Three wheel rotation

Fig. 8 shows the forces working to rotate/pivot the mobile platform around a single stationary wheel (wheel 3 in this case). Wheel 1 has a resultant velocity very close to the direction of the drive motion of the mecanum wheel. Wheels 2 and 4 have motions that are in the  $x$  and  $y$  directions respectively. Their resultant motions must be tangential to the circle about which the mobile platform is rotating. Consider Fig. 8, in this case  $\theta_3 = 0$ . If the vehicle is rotating at an angular velocity  $\dot{\varphi}$  around wheel 3 each point on the vehicle, including wheels 1,2 and 4 must also rotate at  $\dot{\varphi}$  hence:

$$\begin{aligned} \dot{\varphi} &= \frac{\mathbf{v}_1 \sin(\alpha + \xi - 90)}{R_1} \\ &= \frac{\mathbf{v}_{2x'}}{R_2} \\ &= \frac{\mathbf{v}_{4y'}}{R_4} \end{aligned} \quad (25)$$

where  $R_i$  is the distance of wheel  $i$  from the centre of rotation and in this case,  $R_1 = \sqrt{x^2 + y^2}$ ,  $R_2 = \bar{y}$ ,  $R_4 = \bar{x}$  as illustrated in Fig. 8. It can be shown that (25) will apply to other similar configurations with one stationary wheel. In this

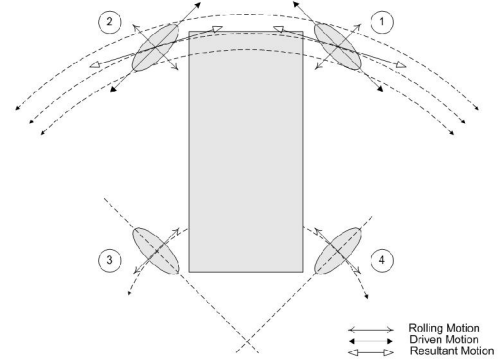


Fig. 9. Rotational motion using two driving wheels

case there is relative motion of the geometric centre in the global  $xy$ -plane given by:

$$\mathbf{v} = \dot{\varphi} R \quad (26)$$

Where  $R = \frac{R_1}{2}$  is the distance between the geometric centre and the centre of rotation. This gives:

$$\dot{x} = \dot{\varphi} R \cos \varphi \quad (27)$$

$$\dot{y} = \dot{\varphi} R \sin \varphi \quad (28)$$

#### C. Two wheel rotation

When turning using only two driving wheels the centre of rotation is determined by the geometry of the non-driven wheels, as they are effectively fixed wheels. As shown in Fig. 9, wheels 1 and 2 are driven with the same rotational direction; wheels 3 and 4 are not driven, however they are free to roll on the roller in contact with the floor. This rolling movement is limited to one line and is tangential to the circle around which the mobile platform is rotating. Wheels 1 and 2 must provide torque for the rotational motion; the force supplied is concentric to the motion of the rollers of wheels 3 and 4. The rollers on wheels 1 and 2 allow them to follow a tangent around the circle at a wider arc. This holds true for any two adjacent driving wheels and it allows rotation around points in front, behind or to either side of the mobile platform. The following equations can be applied to the case illustrated

in Fig. 9, but they can be extended to other cases as explained later, the rotational velocity  $\dot{\varphi}$  can be shown to be:

$$\begin{aligned}\dot{\varphi} &= \frac{\dot{v}_1}{R_1} \\ &= \frac{\dot{v}_2}{R_2}\end{aligned}\quad (29)$$

where  $R_1$  and  $R_2$  are given by

$$R_1 = R_2 = \sqrt{\left(\frac{\bar{x}}{2}\right)^2 + \left(\bar{y} + \frac{\bar{x}}{2} \tan(\alpha)\right)^2} \quad (30)$$

$$R = \frac{\bar{y}}{2} + \frac{\bar{x}}{2} \tan(\alpha) \quad (31)$$

for the case where  $\pm\dot{\theta}_1 = \dot{\theta}_2$ ,  $\dot{\theta}_3 = \dot{\theta}_4 = 0$ . When  $\pm\dot{\theta}_3 = \dot{\theta}_4$ ,  $\dot{\theta}_1 = \dot{\theta}_2 = 0$  use  $R_3$  and  $R_2$  in (29).

When rotation occurs either side of the platform the following wheel rotational velocities are applied,  $\pm\dot{\theta}_1 = \dot{\theta}_4$ ,  $\dot{\theta}_2 = \dot{\theta}_3 = 0$  for rotation about a point to the left of the vehicle in Fig. 9 and  $\pm\dot{\theta}_2 = \dot{\theta}_3$ ,  $\dot{\theta}_1 = \dot{\theta}_4 = 0$  for rotation about a point to the right. For the first case the radii change as follows

$$R_1 = R_4 = \sqrt{\left(\frac{\bar{y}}{2}\right)^2 + \left(\bar{x} + \frac{\bar{y}}{2} \tan(90 - \alpha)\right)^2} \quad (32)$$

$$R = \frac{\bar{x}}{2} + \frac{\bar{y}}{2} \tan(90 - \alpha) \quad (33)$$

in the second case use  $R_2$  and  $R_3$  in (32).

(27) and (28) hold for all the above cases when the correct radii are applied.

## V. RESULTS AND CONCLUSION

The mobile platform's different motions were achieved by a combination of different driven wheels. With four mecanum wheels, 81 different wheel motion combinations could be achieved. For rotational motion, as can be expected, the heading of the mobile platform was changed, however for straight line motions it was possible for the platform to move in any of the predefined directions without having to change its heading. This is important if the mobile platform is going to be successfully deployed in office environments. However some of these combinations produced motions that were not useful, others produced motions that were not predictable due to factors like: slippage due to uneven floor and inconsistent friction on the wheels, wheels that are not aligned with the frame of the vehicle, motors that produce uneven torques, etc. The modelling did not address the behaviour of the mobile platform when using a variation of different speeds on the wheels, that is seen as future work.

The tests performed resulted in 51 functional motions that can be used to manipulate a mecanum wheeled platform, the remaining 30 motions are non-functional motions i.e. they result in no motion of the platform. Non-functional motions results when all the forces and moments produced by all the mecanum wheels are acting opposite each other in such a way that they cancel each others effect. **The developed mathematical models were verified using the mobile platform's integrated motion sensor system.**

TABLE I  
WHEEL ROTATIONS FOR TRANSLATIONAL MOTION

| Wheel Number | 1 | 2 | 3 | 4 |
|--------------|---|---|---|---|
| Direction    |   |   |   |   |
| North        | + | + | + | + |
|              | + | + | 0 | 0 |
|              | 0 | 0 | + | + |
| South        | - | - | - | - |
|              | - | - | 0 | 0 |
|              | 0 | 0 | - | - |
| East         | - | + | - | + |
|              | - | 0 | 0 | + |
|              | 0 | + | - | 0 |
| West         | + | - | + | - |
|              | + | 0 | 0 | - |
|              | 0 | - | + | 0 |
| North-east   | 0 | + | 0 | + |
| South west   | 0 | - | 0 | - |
| Northwest    | + | 0 | + | 0 |
| South-east   | - | 0 | - | 0 |

## APPENDIX

Table I the rotational directions required for the basic translational motions, for further information on rotational and non-functional motions please contact the authors. The wheels are numbered simply 1-4, refer to Fig. 7 for the convention used for numbering the wheels. Once again for clarity translational directions will be described as points of the compass.

## REFERENCES

- [1] Kalpakjiaan S, Schmid SR. *Manufacturing Engineering and Technology*, 4th Edition, Prentice Hall, USA, 2000
- [2] West M, Asada H. *Design of Ball Wheel Mechanisms for Omni-directional Vehicles with Full Mobility and Invariant Kinematics* Journal of Mechanical Design 1997; 119:153-61
- [3] Dickerson SL, Lapin DB. *Control of Omni-Directional Robotic Vehicle with Mecanum Wheels*. IEEE Proceedings of National Tele-systems Conference 1991;323-8.
- [4] Tlale NS. *On Distributed Mechatronic Controller for Omni-Direction Autonomous Guided Vehicles*. Industrial Robot: An International Journal 2006; 33(4):278-84
- [5] Badve AA. *All Terrain Omni-Directional Autonomous Mobile Robot*. Master's Thesis, Massey University, Auckland, New Zealand 2003
- [6] Shimada A, Yajima S, Viboonchaicheep P, Samura K. *Mecanum-wheel vehicle systems based on position corrective control*. 32nd Annual Conference of IEEE Industrial Electronics Society 2005; 2077-82.
- [7] Tahboub KA, Asada HH. *Dynamics analysis and control of holonomic vehicle with a continuously variable transmission*. Proceedings of the IEEE International Conference on Robotics and Automation 2000; 3:2466-72.
- [8] Viboonchaicheep P, Shimada A, Kosaka Y. *Position rectification control for mecanum wheeled omni-directional vehicles*. 29th Annual Conference of IEEE Industrial Electronics Society 2006; 854-59.
- [9] Bright G, Potgieter J, Tlale S, Deigel O. *Control of a Domestic Mobile Robot Using Wireless LAN via the Internet*, 18th International Conference on CAD/CAM, Robotics and Factories of the Future, Kuala Lumpur, Malaysia, 2003; pp. 655-660.